Design and demonstration of multimodal optical scanning microscopy for confocal and two-photon imaging

Wanhee Chun, Dukho Do, and Dae-Gab Gweon

Related Articles

Cantilever-based optical interfacial force microscope in liquid using an optical-fiber tip
AIP Advances 3, 032126 (2013)

Material-based three-dimensional imaging with nanostructured surfaces
Appl. Phys. Lett. 102, 011116 (2013)

Far-field super-resolution imaging using near-field illumination by micro-fiber
Appl. Phys. Lett. 102, 013104 (2013)

New Products
Rev. Sci. Instrum. 83, 129501 (2012)

Confocal sample-scanning microscope for single-molecule spectroscopy and microscopy with fast sample exchange at cryogenic temperatures
Rev. Sci. Instrum. 83, 123706 (2012)
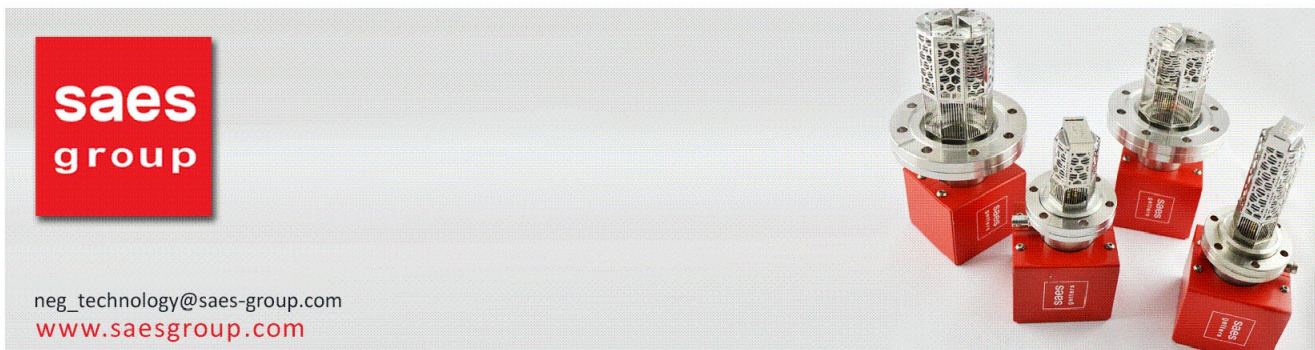
Additional information on Rev. Sci. Instrum.

Design and demonstration of multimodal optical scanning microscopy for confocal and two-photon imaging

Wanhee Chun, Dukho Do, and Dae-Gab Gweon
Department of Mechanical Engineering, KAIST, Daejeon 305-701, South Korea

We developed a multimodal microscopy based on an optical scanning system in order to obtain diverse optical information of the same area of a sample. Multimodal imaging researches have mostly depended on a commercial microscope platform, easy to use but restrictive to extend imaging modalities. In this work, the beam scanning optics, especially including a relay lens, was customized to transfer broadband (400–1000 nm) lights to a sample without any optical error or loss. The customized scanning optics guarantees the best performances of imaging techniques utilizing the lights within the design wavelength. Confocal reflection, confocal fluorescence, and two-photon excitation fluorescence images were obtained, through respective implemented imaging channels, to demonstrate imaging feasibility for near-UV, visible, near-IR continuous light, and pulsed light in the scanning optics. The imaging performances for spatial resolution and image contrast were verified experimentally; the results were satisfactory in comparison with theoretical results. The advantages of customization, containing low cost, outstanding combining ability and diverse applications, will contribute to vitalize multimodal imaging researches. © *2013 American Institute of Physics*. [http://dx.doi.org/10.1063/1.4773232]

I. INTRODUCTION

Light is a valuable tool to access not only structural information but also information on biochemical properties. The amount of reflection and fluorescent light, and the characteristics of temporal and spectral changes of those lights provide various information of the bio-specimen.[1] An optical scanning microscope approaching a sample point by point is appropriate to visualize these optical signals. Confocal imaging for reflection and fluorescence,[2] nonlinear imaging such as two-photon excitation[3] and high harmonic generation imaging,[4] spectral imaging for wavelength transition,[5] and fluorescence lifetime imaging[6] are representative imaging techniques realized within the framework of the optical scanning microscope. If all kinds of image information of such imaging systems are synthesized, the weaknesses of each other will be complemented and the reliability of analytic results will be improved.[7] However, there are limits to put together image information obtained from independent microscopes, because the small views of the instruments are very difficult to be matched. Therefore a multimodal microscope is required, sharing the principal optical elements of instruments. The multimodal microscopy facilitates to obtain various images for the specific area of a sample and has an effect of cost reduction. Until now, researches on the multimodal imaging have been mainly reported on the basis of a commercial confocal microscope or commercial lens platform.[8–11] Although the commercial systems are easy and stable to handle, all of the imaging lights in wide wavelength may be not considered in development of the commercial platforms. This fact slows down the performance of multimodal imaging and restricts to extend imaging modalities.

In this paper, we report the development of an optical scanning microscope, as a substitute for commercial instruments, for the multimodal imaging. Especially, a relay lens is required to transfer scanning beams without optical error, aberration, and loss in the scanning optics. In the past, a relay lens with high quality was proposed to be utilized in confocal scanning system.[12] For multimodal imaging, advanced relay lens needs to be customized for the lights of wide wavelength, used for most imaging techniques. Confocal reflection, confocal fluorescence, and two-photon excitation fluorescence images are obtained to demonstrate imaging feasibility in the customized scanning platform. Point spread function is measured to verify the imaging performances of respective imaging techniques, as representative imaging techniques using near-ultraviolet (NUV), visible, near-infrared (NIR), and pulsed lights. In summary, this paper focuses on the optical design, the configuration proposal, and the experimental demonstration for the multimodal imaging combining confocal and two-photon imaging.

II. CONFIGURATION PRINCIPLES

Figure 1 shows the proposed configuration of the multimodal optical scanning microscope. First of all, the beam scanning components of confocal reflectance, confocal fluorescence, and two-photon fluorescence imaging instruments are shared in the configuration. Three independent imaging parts built around the shared beam scanning optics access a sample along the common optical path. The collimated beams from NIR laser (LASER1, 830 nm Diode laser, Blue Sky Research), RGB laser (LASER2, He-Ne 543 nm laser, He-Ne 633 nm laser, Argon ion 488 nm laser, Coherent Inc.), and ultrafast pulsed laser (LASER3, 780 nm, 130 fs laser, Toptica) are transferred to the beam scanning optics together. The beam scanning optics generates multimodal optical probes, movable focal spots, at the same position and collects light signals regarding sample information. The mirror scanner
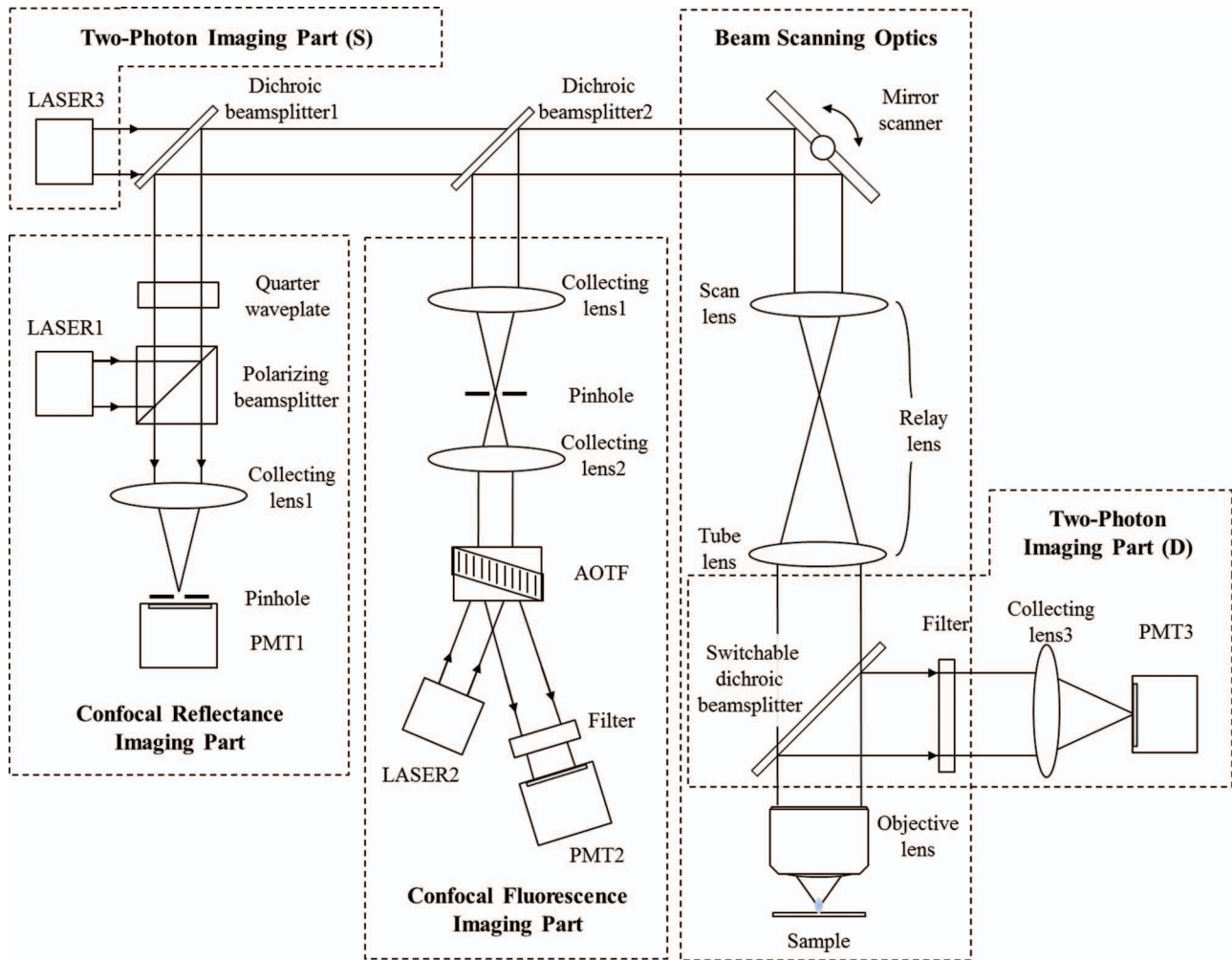
FIG. 1. The schematic diagram of the configuration of multimodal optical scanning microscope.

(6210h galvano mirror, Camtech), composed of two scanning mirrors crossed orthogonally, determines scanning position by adjusting focal position according to the angle of the lights. The light signals that return to allocated detecting channels (PMT 1-3, Hamamatsu) are converted into images with the scanning position. The reflection and fluorescent lights for the confocal imaging are filtered by a pinhole and a collecting lens1; the fluorescent light for the two-photon imaging is gathered to the aperture of PMT3 by a collecting lens 3.

It is also important to create the optical paths to combine or separate the imaging lights, as shown in Figs. 1 and 2. The illumination and excitation beams with wavelength differences are easily put together by dichroic beamsplitters (1, 2) before proceeding to the beam scanning optics. In
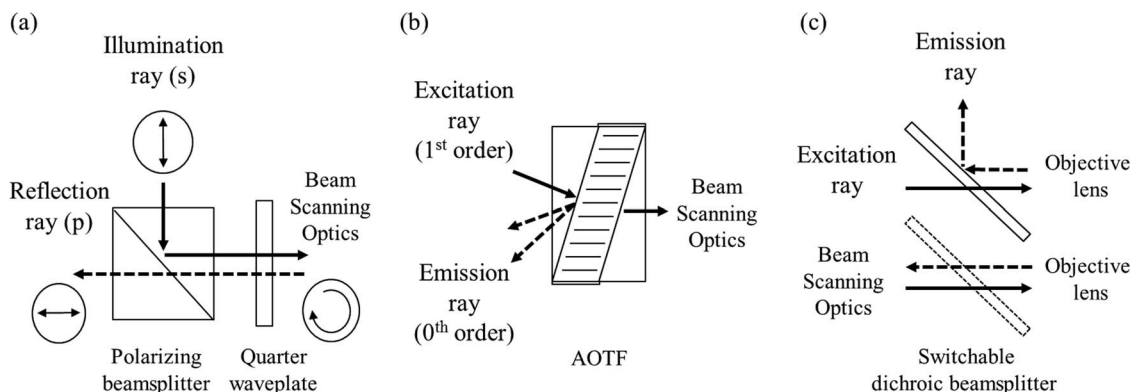

FIG. 2. The principles of beam splitters. (a) Illumination/reflection rays separated by PBS and QWP. (b) Excitation/emission rays separated by AOTF. (c) Excitation/emission rays separated by SDBS.

confocal reflectance imaging part, a polarizing beam splitter (PBS) can separate the light reflected or scattered at a sample and the illumination light due to the changes of their polarization state. The polarization state of the reflection light are changed from s-polarization to p-polarization, while passing a quarter wave plate (QWP), which induces the phase retardation of a quarter-wavelength, twice. A fluorescent emission light can be distinguished from excitation light due to wavelength changes caused by Stokes shift. The confocal fluorescence imaging employs an acousto-optical tunable filter (AOTF, TF550-300, Gooch & Housego Inc.) to arrange excitation rays and emission rays flexibly, conveniently, and efficiently, instead of a dichroic beamsplitter with a fixed edge which is not sufficient for overlapped wavelength spectra of various fluorophores. AOTF, birefringent crystal with an RF wave,[13] diffracts the light of the wavelength selected by the RF signal of the specific frequency. The excitation light diffracted to the 1st order route travels between the beam scanning optics and the light source; the fluorescent emission light of the wavelength band except for the narrow diffraction band propagates to the detecting channel along the 0th order route. The emission rays of the 0th order may have problems regarding dispersion, divergence, and separation by birefringence generally. As a similar case, acousto-optical beam splitter of Leica Corp. compensates the problems by another birefringence material.[14] The configuration to locate pinhole filtering optics between the mirror scanner and AOTF and the detector close to AOTF can ignore the effects which results from those problems without additional elements. Furthermore, the pinhole filtering optics eliminates the artifacts induced by the aberration of AOTF and controls the beam size to relay the apertures of the mirror scanner and AOTF. The light emitted from fluorophores excited by the two-photon absorption effect is detected before being de-scanned by the mirror scanner, because the emission signals generated inside the only focal volume does not need to be filtered. A switchable dichroic beamsplitter (SDBS) between the mirror scanner and objective lens is operated occasionally for the two-photon imaging, except for the confocal imaging mode of which emission spectra are overlapped.

The system configuration is cost-effective and easy to combine imaging modalities by sharing the principal components. Not only the above-mentioned imaging modes but also other imaging modes based on beam scanning system can be realized easily in the configuration. In order to extend the imaging modalities, the illumination and detection parts for respective imaging are added to the beam scanning optics, but within optical acceptance criteria. Therefore, an optical design is required to cover broadband imaging lights; the details are described in Sec. III.

III. DESIGN OF LENS SYSTEM

The optical error, aberration and loss of the scanning optics degrade qualities of a resultant image: optical resolution, signal-to-noise ratio (SNR), and image contrast. Chromatic aberration principally results in performance deterioration of multimodal imaging. The imaging lights, which contain the

TABLE I. The specifications for the design requirements of relay lens.

Wavelength	400–1000 nm
Input beam diameter (mirror scanner)	5 mm
Output beam diameter (objective lens)	15 mm
Magnification factor	×3
Field angle@objective lens	+/− 2.7°
Scanning angle@mirror scanner	+/−8.1°
Field of view (20× objective lens)	$600 \times 600 \ \mu m^2$

illumination, reflection, excitation, and emission light, range in wavelength from 400 to 1000 nm. The relay lens of the beam scanning optics should be corrected optically for the broadband wavelength.

The role of the relay lens, which consists of a scan lens and tube lens, is to transfer the scanning beams between the mirror scanner and the objective lens without optical vignetting.[12] The relay lens needs to satisfy double-telecentric 4-f condition and the diffraction-limit criterion. The double telecentric condition, in which both entrance and exit pupils are located at infinity, produces a collimated beam suitable for the beam scanning mechanism. The 4-f condition, which places the mirror scanner at the front focal plane of the scan lens and the objective lens at the back focal plane of the tube lens, keeps scanning beams within the aperture bounds of the mirror scanner and the objective lens. Furthermore, the relay lens should expand a collimated beam in order to fill the back aperture of the objective lens from the collimated beam limited by the aperture size of the mirror scanner. The magnification factor of the relay lens is determined by the ratio of focal lengths of the tube lens (f_t) to scan lens (f_s). The value of the ratio also affects the field angle of the beams delivered to the objective lens, which determines field of view of the scanning microscope.

The specific requirements of the relay lens are listed in Table I. The design wavelength is a range from 400 to 1000 nm, considering fluorescence excitation/emission light (400–700 nm), reflection imaging light (830 nm), and candidate of ultrafast pulsed laser sources (800–1000 nm). The magnification factor is determined to be three, for the aperture diameters of the mirror scanner and objective lens are 5 and 15 mm, respectively. The focal position (p) away from the center on the specimen is expressed as the following equation,

$$p = f_o \tan \left(\theta_s / M \right), \tag{1}$$

where f_o, θ_s, and M are the focal length of objective lens, the scanning angle by mirror scanner, and the magnification factor of relay lens. According to Eq. (1), the maximum values of the field angle at the back aperture of objective lens and the scanning angle by mirror scanner are determined to be ±2.7° and ±8.1°, respectively, in order to view an area up to 600 μm square with 20× objective lens.

The scan lens and tube lens were designed individually for convenience of optimization. Before iteration for optimization, doublet and triplet lens configuration were referred as starting points of a design process. The doublet and triplet lens are used generally to correct chromatic aberration by using glasses with different amounts of dispersion. A beam
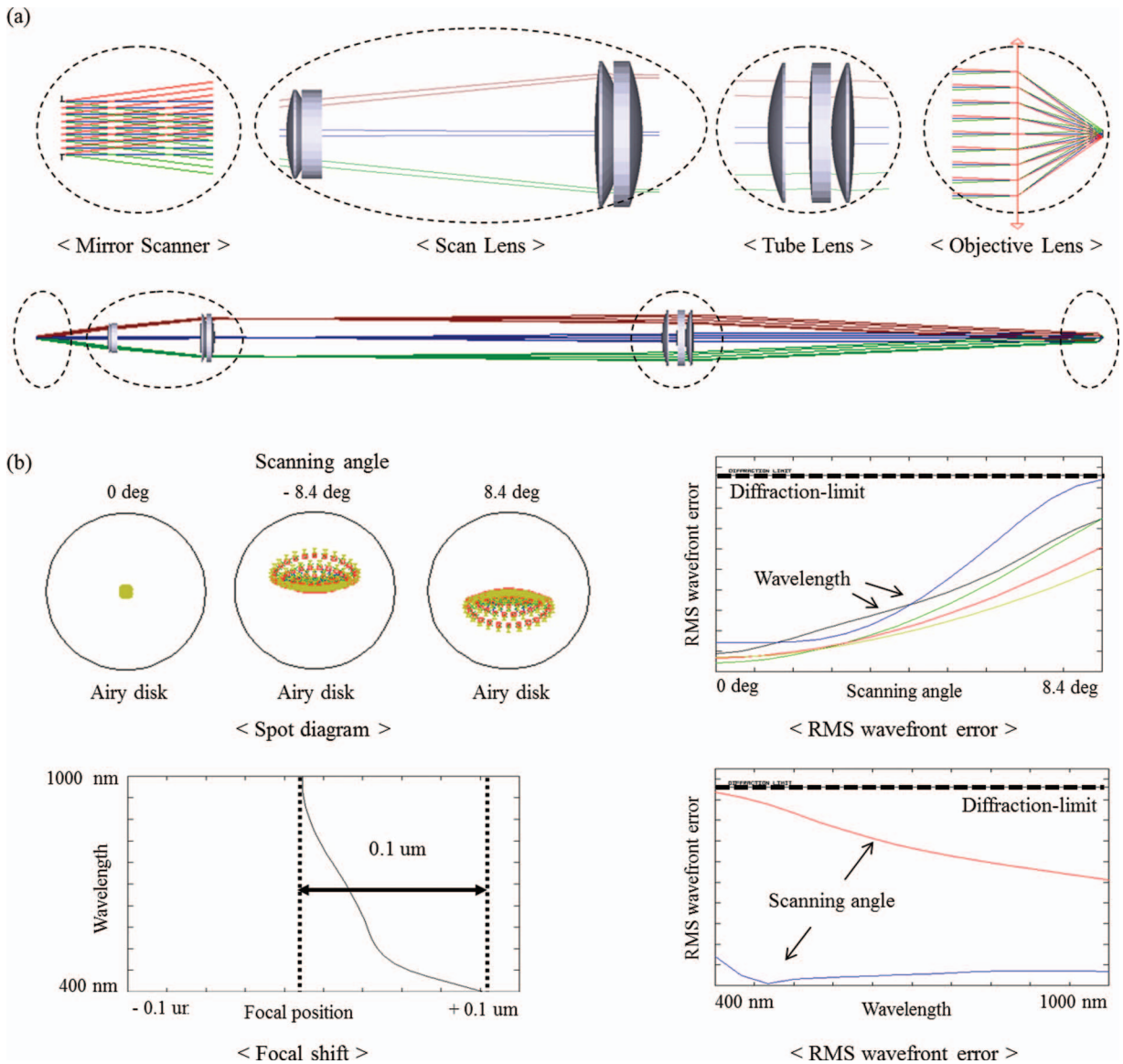
FIG. 3. The design results of relay lens. (a) The lens configuration with the traced rays. (b) The performance analysis (spot diagram: the distribution of each image point for the respective scanning beams (from −8.4° to 8.4°), rms wavefront error: the deviation of aberrated wavefront from the ideal wavefront as a function of scanning angle (0, 8.4°) and wavelength (400–1000 nm), Focal shift: the differences of the focal position for wavelength (400–1000 nm), which occurs due to chromatic aberration, with respect to paraxial focus of the primary wavelength).

entering the scan lens is smaller in size and larger in field angles than that of the tube lens. The scan lens which requires a high refractive power to refract rays with the large field angle was configured of two doublet lenses initially. The optimal design of the tube lens was started from a triplet configuration to be appropriate for the large beam size. The curvature of spherical surfaces, the distance between surfaces, and the glass material of the lens were established by variables and optimized to reduce a cost function. The wavefront induced by optical aberrations is deformed; the root-mean-square (rms) value of the differences from the ideal wavefront is taken as the cost function. The optimization of the variables was iterated to reduce the cost function for all scanning rays, within the boundaries of the aforementioned requirements.

The beam scanning optics with the designed lens is configured to evaluate its performance, as shown in Fig. 3. The scan lens and the tube lens designed separately are combined and a perfect lens replaces an objective lens. The ray-tracing results and the expected performance of the relay lens system are analyzed in Figs. 3(a) and 3(b). The scanning rays with the angle of incidence and the broad wavelength are corrected well and transferred between the apertures of the devices without optical vignetting. The spot diagram indicates the satisfactory focal distribution that all the foci of the scanning beams are located in the Airy disk related to the inherent diffraction characteristic. The rms wavefront error curves for the design angle and wavelength are always below the diffraction-limit level (0.07 waves) of the optical design criterion by Maréchal.[15] The focal shift curve shows the appropriate correction level of chromatic aberration that the deviation is very small in comparison to the value of the axial resolution of several micrometers.

The design result satisfies all of the requirements of the relay lens and the design criterions of the diffraction limit, for

the design wavelength (400–1000 nm) broader than the existing capacity of a commercial platform. A functional error of relay lens, optical error induced by optical aberrations, and light loss by absence of antireflection coating can be serious problems to realize the multimodal imaging in a commercial platform. The satisfactory results of the design guarantee the best imaging performances in the customized platform and facilitate to combine various imaging techniques based on scanning system. Not only the proposed imaging techniques but also other imaging techniques utilizing the lights within the design wavelength, such as multispectral two-photon imaging and NIR fluorescence imaging, are expected to be realized appropriately in this platform.

IV. EXPERIMENTAL RESULTS

We demonstrated the imaging feasibility for NUV, visible, NIR continuous light, and NIR pulsed light in the platform equipped with the designed relay lens. The imaging parts were built around the beam scanning optics to ob-tain confocal fluorescence, and two-photon excitation fluorescence images, respectively. The performances were evaluated from the images obtained by the multimodal imaging system.

The point spread function (PSF), which represents optical resolution, was measured from an image for very tiny fluorescent beads of 45 nm diameter (Invitrogen F10720); a sub-resolution sized particle can be assumed to a point object.[16] A 50× objective lens (NA 0.8) and a pinhole near to size of the Airy disk were utilized. The lateral and axial sectional images for confocal and two-photon fluorescence imaging are shown with their cross section profiles in Fig. 4. The theoretical PSF is displayed with the measured PSF for comparison, following the experimental condition and assuming a Stokes shift of 1.2. The theoretical PSF of those imaging techniques is expressed as the following equation:

$$h_{confocal}(r) = h_{illu}(r)\{h_{det}(r) \otimes D(r)\}, \qquad (2)$$

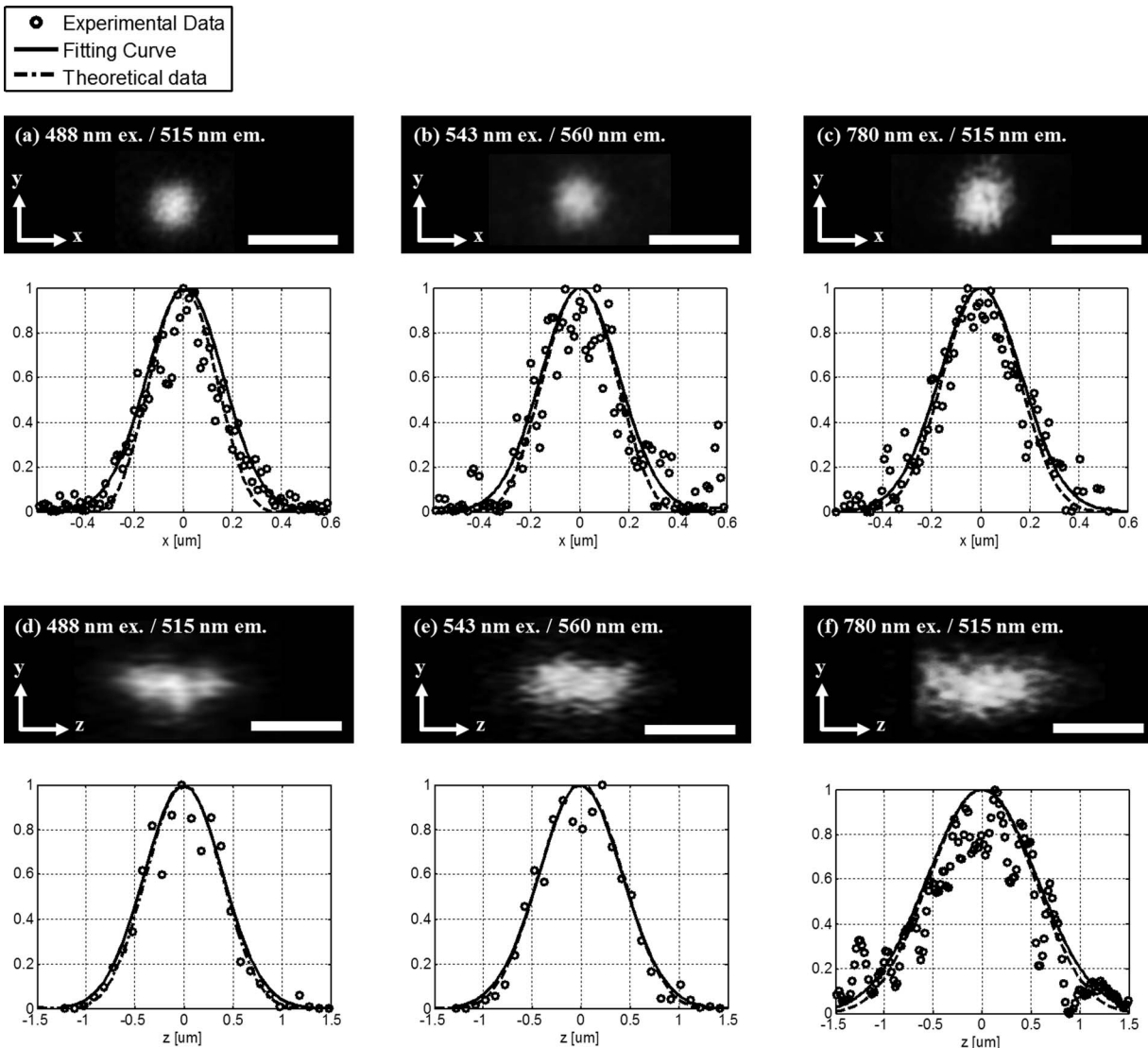$$h_{two-photon}(r) = [h_{illu}(r)]^2, \qquad (3)$$

FIG. 4. The images and the section profiles (experimental and theoretical results) of lateral and axial point spread function (PSF). The scale bar in the figure represents 1 μm.

TABLE II. Experimental and theoretical results of full width at half maximum (FWHM) of lateral and axial point spread function (PSF).

FWHM of PSF		Confocal imaging (488 nm excitation) (nm)	Confocal imaging (543 nm excitation) (nm)	Two-photon imaging (780 nm excitation) (nm)
Lateral	Expt.	368	378	397
PSF	Theory	310	346	365
Axial	Expt.	933	998	1320
PSF	Theory	868	966	1260

where $h_{illu}(r)$, $h_{det}(r)$, and $D(r)$ are point spread function of illumination optics and detection optics, and pinhole pupil function, respectively.[17–19] The values of full width at half maximum (FWHM) of theoretical and measured point spread function are listed in Table II. The result indicates that the imaging techniques have the satisfactory performance, respectively, although being operated within the unified system. In other words, the result verifies that the developed system is designed well for the imaging lights. Other imaging techniques using the lights within the design wavelength may have also the spatial resolution to the same level.

Figure 5 shows the multimodal images for the tissue slice of mouse kidney and mouse liver. The cellular components of the tissue were labeled with Alexa Fluor 488 WGA (peak excitation at 499 nm, emission maximum at 520 nm), Alexa Fluor 568 Phalloidin (peak excitation at 578 nm, emission at 603 nm), and DAPI (peak excitation at 359 nm, emission maximum at 461 nm). The multimodal images containing different and similar information for the same area of a sample were obtained by respective imaging techniques with a 20× objective lens (NA 0.75). The cellular structures are recognized in the confocal reflection image (a). The lights are scattered or reflected mostly at the cell boundaries, at which the refractive index is changed. This is applicable to structural
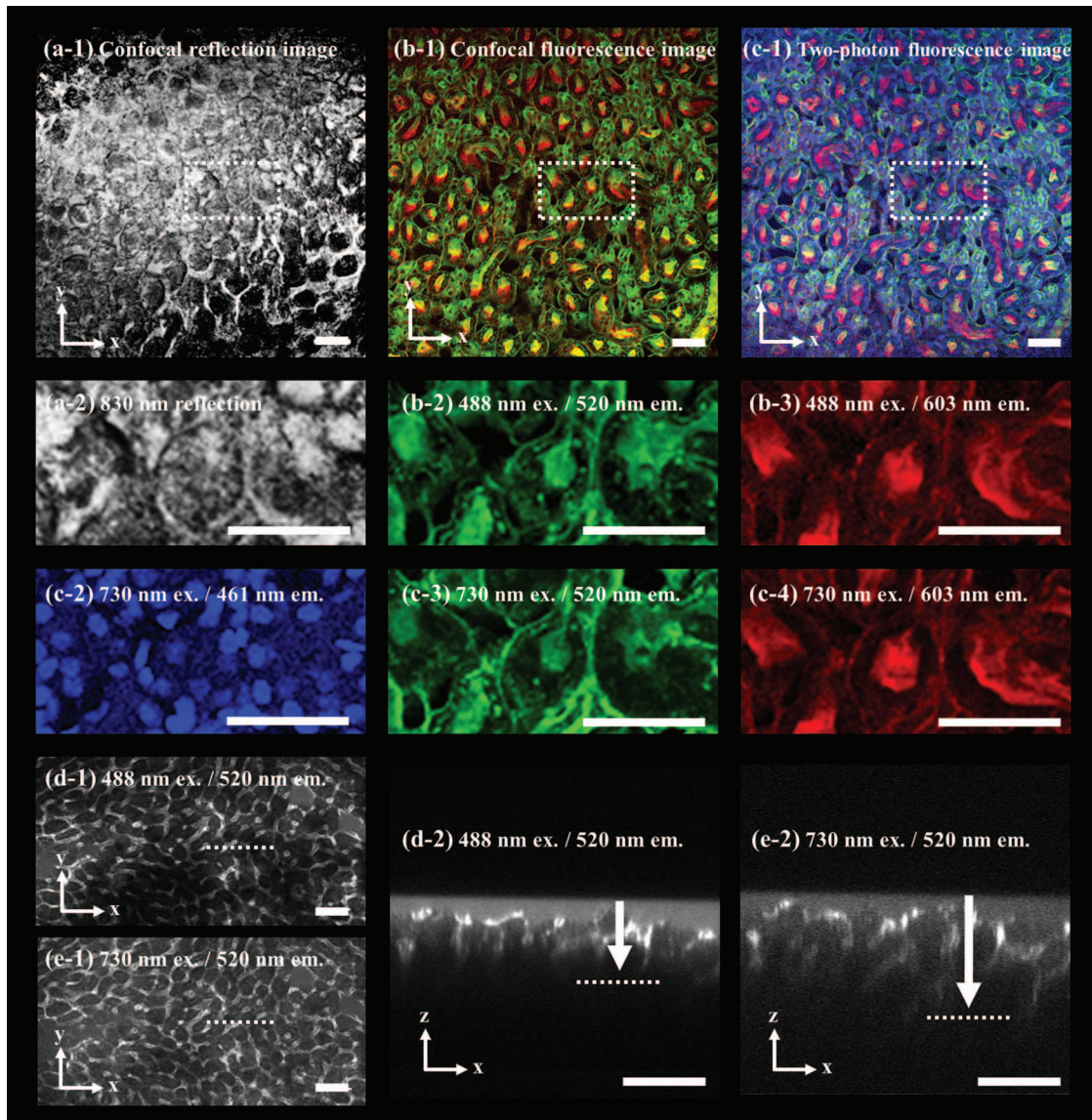

FIG. 5. (a) Confocal reflectance image. (b, d) Confocal fluorescence image. (c, e) Two-photon fluorescence image of the tissue slice. The scale bar in the figure represents 50 μm.

analyses that do not need or are not suitable for fluorescent labeling. However, lights scattered indiscriminately at tissue surface make the cell structure difficult to be distinguished clearly; this symptom appears at the center of the surface closest to the focal plane. Confocal fluorescence images (b, d) and two-photon fluorescence images (c, e) show the similar results for the cytoplasmic structures (cell wall and membrane) information. The images were obtained individually according to emission band of the fluorescent dyes; their magnified images (b2-3, c2-4) and merged images (b-1, c-1) are displayed. The characteristics of high image contrast and similarity assure that both imaging modes are operated successfully in the customized platform. These imaging modes can be applied to obtain targeted information separately, e.g., the respective analysis for changes of each cellular component. The multimodal imaging of them facilitates to complement the pros and cons of the imaging modes each other according to circumstances. Confocal imaging has an advantage in regards to fluorescent dyes with low yield. Confocal imaging can acquire high signal level of the fluorescent emission through high intensity excitation, from continuous LASERs of various wavelength and low cost. On the contrary, light sources of a broadband femtosecond pulsed beam, required to excite almost fluorophores through the two-photon absorption,[20] are not easy to be utilized, because they are exceedingly expensive. However, femtosecond pulsed beam of single wavelength can excite several fluorescent dyes simultaneously due to the extended spectra of two-photon excitation. Two-photon imaging is replaceable to confocal imaging in the unimportant case of signal level and more favorable to depth imaging than that. A pulsed beam of NIR wavelength penetrates the tissue about 1.5 times deeper than does a visible beam, like the arrows in axial section images (d-e, e-2) corresponding to the dotted line of the lateral section image (d-1, e-1), because NIR light is less absorbed in the medium.[21] Additionally, nonlinear effect of the two-photon imaging limited to focal volume reduces the effects of photo-bleaching and autofluorescence background signal on the surrounding regions.[22] Two-photon imaging is appropriate for live cell imaging, which requires long-term exposure; SNR of an image is high despite signals of low signal level. The resultant images obtained through the customized platform verified the performances and confirmed the complementary relationships among the imaging techniques.

V. CONCLUSION

A beam scanning platform for multimodal imaging was customized to substitute a commercial instrument. A relay lens was designed so that the imaging lights of wide wavelength could be transferred without optical aberration in the beam scanning optics. The design result of the relay lens which satisfies the requirements guarantees the best imaging performances on a design aspect. Various imaging techniques using the lights within the design wavelength are more feasible in the customized platform than a commercial instrument. The multimodal microscopy combining the imaging techniques can be configured easily and cost-effectively by adding respective light sources and detectors to the beam

scanning platform. The imaging parts were implemented to the beam scanning optics to demonstrate confocal reflectance imaging, fluorescence imaging, and two-photon fluorescence imaging. A polarizing beam splitter, dichroic beam splitters, and an acousto-optical tunable filter arrange the optical paths of the imaging lights for illumination, reflection, excitation, and fluorescence emission. The images for the same area of a sample were obtained to verify imaging feasibility for near-ultraviolet, visible, near-infrared continuous light, and pulsed light in the scanning optics. Reflectance images for lights scattered on structure boundaries and fluorescent images emitted from specific targets of a sample were compared each other. The performances results of point spread function and image contrast measured in the customized platform were satisfactory, although the imaging techniques were combined. These results support outstanding combining ability for imaging techniques utilizing the broadband lights within the design wavelength.

Not only the three imaging modes but also other imaging modes will be added to the customized platform through future researches. The design result and the experimental feasibility of the customized platform give other imaging techniques the potential to be realized to the same level. Multimodal imaging through additional combination will contribute to improve the reliability of analytic results and vitalize research areas of bio-medical application. We plan to realize spectral imaging from a visible light, fluorescence lifetime imaging, high harmonic generation imaging for an ultrafast pulsed light, etc. in the developed system.

[1]P. N. Prasad, *Introduction to Biophotonics* (Wiley, Hoboken, NJ, 2003).
[2]D. M. Shotton, J. Cell. Sci. **94**, 175–206 (1989).
[3]K. Konig, J. Microsc.-Oxf. **200**, 83–104 (2000).
[4]W. R. Zipfel, R. M. Williams, R. Christie, A. Y. Nikitin, B. T. Hyman, and W. W. Webb, Proc. Natl. Acad. Sci. U.S.A. **100**(12), 7075–7080 (2003).
[5]T. Zimmermann, J. Rietdorf, and R. Pepperkok, FEBS Lett. **546**(1), 87–92 (2003).
[6]E. B. van Munster and T. W. J. Gadella, in *Microscopy Techniques*, edited by J. Rietdorf (Springer-Verlag, Berlin, 2005), Vol. 95, pp. 143–175.
[7]M. J. Koehler, M. Speicher, S. Lange-Asschenfeldt, E. Stockfleth, S. Metz, P. Elsner, M. Kaatz, and K. Konig, Exp. Dermatol. **20**(7), 589–594 (2011).
[8]M. Mathew, S. Santos, D. Zalvidea, and P. Loza-Alvarez, Rev. Sci. Instrum. **80**(7), 073701 (2009).
[9]H. T. Chen, H. F. Wang, M. N. Slipchenko, Y. K. Jung, Y. Z. Shi, J. B. Zhu, K. K. Buhman, and J. X. Cheng, Opt. Express **17**(3), 1282–1290 (2009).
[10]I. Veilleux, J. A. Spencer, D. P. Biss, D. Cote, and C. P. Lin, IEEE J. Sel. Top. Quantum Electron. **14**(1), 10–18 (2008).
[11]W. C. Warger, G. S. Laevsky, D. J. Townsend, M. Rajadhyaksha, and C. A. DiMarzio, J. Biomed. Opt. **12**(4), 044006 (2007).
[12]A. C. Ribes, S. Damaskinos, and A. E. Dixon, Scanning **22**(5), 282–287 (2000).
[13]I. C. Chang, IEEE Trans. Sonics. Ultrason. **23**(1), 2–22 (1976).
[14]V. Seyfried, H. Birk, R. Storz, and H. Ulrich, "Advances in multispectral confocal imaging," *Proc. SPIE 5139*, Confocal, Multiphoton, and Nonlinear Microscopic Imaging, 147 (October 10, 2003).

[15]W. J. Smith, *Modern Optical Engineering: The Design of Optical Systems*, 4th ed. (McGraw-Hill, New York, 2008).

[16]H. Yoo, I. Song, and D. G. Gweon, J. Microsc.-Oxf. **221**, 172–176 (2006).

[17]M. Gu and C. Sheppard, J. Microsc. **177**(2), 128–137 (1995).

[18]M. Gu, *Principles of Three Dimensional Imaging in Confocal Microscopes* (World Scientific, Singapore/River Edge, NJ, 1996).

[19]G. Cox and C. J. R. Sheppard, Microsc. Res. Tech. **63**(1), 18–22 (2004).

[20]M. E. Dickinson, E. Simbuerger, B. Zimmermann, C. W. Waters, and S. E. Fraser, J. Biomed. Opt. **8**(3), 329–338 (2003).

[21]V. E. Centonze and J. G. White, Biophys. J. **75**(4), 2015–2024 (1998).

[22]Y. Sako, A. Sekihata, Y. Yanagisawa, M. Yamamoto, Y. Shimada, K. Ozaki, and A. Kusumi, J. Microsc.-Oxf. **185**, 9–20 (1997).